

# A Model for the Random Video Process

By L. E. FRANKS

(Manuscript received December 27, 1965)

*For problems concerning the transmission of video signals, it is often desirable to know the statistical distribution of power in the frequency domain for the signal process. It is convenient to have a model, involving only a few essential parameters, which will satisfactorily characterize the power spectral density of the random video signal. This paper proposes a model for the random picture and derives expressions for second-order statistical properties of the video signal obtained from a conventional scanning operation on the picture. The properties of typical picture material make valid certain approximations which lead to especially simple, closed-form expressions for power spectral density. The continuous part of the power spectral density is expressed as a product of three factors, characterizing separately the influence of point-to-point, line-to-line, and frame-to-frame correlation. For parameters representative of typical picture material there is observed an extreme concentration of power near multiples of the line scan and frame scan rates. An illustrative example of the use of the model in an optimum linear filtering problem is included.*

## I. INTRODUCTION

This paper provides a detailed development of a simple model for characterizing the statistical properties of a random video signal. The primary concern is the modeling of the power spectral density of the electrical process generated by linear, sequential scanning of a rectangular portion of an infinite, two-dimensional random picture. The spatial and temporal statistical properties of typical picture material allow approximations which lead to a model having an especially simple form, characterized by only a few parameters. The model has a form convenient for the analysis of a variety of signal transmission problems. The validity of the model for these purposes is established by comparing it with results obtained in several independent experimental studies.<sup>1,2,3</sup>

The relationship between the second-order statistics of the random picture and those of the resulting video signal due to line-to-line and

frame-to-frame correlation is examined in Section II. Section III considers the composite video signal wherein the picture signal is periodically interrupted and a periodic pattern is inserted for purposes of synchronization and blanking. A model of the random picture process is developed in Section IV. The results are combined in Section V to provide a summary of expressions for the power spectral density of the composite video signal. Section VI is an illustrative example of the use of the model for deriving optimum linear signal processing networks for video signal transmission over a noisy channel. A glossary of symbols is provided in Appendix A.

## II. EFFECTS OF THE SCANNING OPERATION

For the first step in the development of the random video signal, we consider a still picture with luminance given by the "stationary" random process,  $d(x,y)$ ; i.e., the two-dimensional autocovariance function for the process can be described by

$$E [d(x_1, y_1) d(x_2, y_2)] = \varphi(\alpha, \beta), \quad (1)$$

where  $\alpha = x_2 - x_1 =$  horizontal displacement

$\beta = y_2 - y_1 =$  vertical displacement.

For convenience in derivation of the equations, we assume that  $d(x,y)$  is a zero-mean process. Although physically  $d(x,y)$  would be non-negative, it is easier to add in the mean in the final expressions. The video signal,  $v(t)$ , at the output of an optical scanner moving at constant velocity across the picture is a stationary process with an autocorrelation function simply related to  $\varphi(\alpha, \beta)$ . In order to avoid the introduction of unnecessary constants, assume that the scanner moves in a horizontal direction at unit velocity and also that output voltage is proportional to luminance with unit conversion gain. Then

$$\varphi_1(\tau) = E[v(t)v(t + \tau)] = \varphi(\tau, 0)$$

and

$$E[v(t)] = 0. \quad (2)$$

Actually, the scanner output is normally a nonlinear function of luminance, however, the model developed here has the property that its autocovariance function is changed only by a multiplicative constant when subjected to a zero-memory, nonlinear transformation.\* Hence, the model remains valid for any scanner characteristic and any in-

\* For the random process described in Section IV, the autocovariance is proportional to the variance of the first-order amplitude probability density function.

stantaneous companding operation to which the video signal might be subjected.

The next step is to account for the effects of line-to-line correlation by considering the sequential scanning of a still picture in the form of an infinite strip with a finite horizontal width, traversed by the scanner in an interval of  $T$  seconds. Successive lines are separated in a vertical direction by a distance corresponding to the horizontal travel of the scanner in an interval of  $T_e$  seconds. The abrupt change in scanner position when it reaches the edge of the strip causes the video signal to be a nonstationary process. The autocorrelation for the process,  $\psi(t, \tau) = E[v(t)v(t + \tau)]$  is periodic  $T$  in  $t$ . This is related to a stationary process in the usual manner by considering  $t$  a random variable uniformly distributed over the interval  $(0, T]$ . Then,

$$\begin{aligned}\varphi_2(\tau) &= E[\psi(t, \tau)] \\ &= \sum_{k=-\infty}^{\infty} \varphi(\tau - kT, kT_e) P(k, \tau).\end{aligned}\quad (3)$$

The probability,  $P(k, \tau)$ , that the points  $t$  and  $t + \tau$  fall in lines  $k$  apart is given by the translates of the triangular function,  $q_T(\tau)$ .

$$P(k, \tau) = q_T(\tau - kT),$$

where

$$\begin{aligned}q_T(\tau) &= 1 - \frac{|\tau|}{T} \quad \text{for } |\tau| \leq T \\ &= 0 \quad \text{otherwise.}\end{aligned}\quad (4)$$

Combining (3) and (4), the autocorrelation function for the video signal with line-to-line correlation taken into account becomes

$$\varphi_2(\tau) = \sum_{k=-\infty}^{\infty} \varphi(\tau - kT, kT_e) q_T(\tau - kT), \quad (5)$$

For typical picture material,  $\varphi(T/2, \beta) \cong 0$ . In this case  $\varphi_2(\tau)$  is a sequence of essentially isolated pulse shapes,  $q_T(\tau)\varphi(\tau, 0)$ , centered on integral multiples of  $T$ , the  $k$ th pulse from the origin having a magnitude proportional to  $\varphi(0, kT_e)$  as indicated in Fig. 1.

The power spectral density of this process is

$$\begin{aligned}\Phi_2(f) &= \int_{-\infty}^{\infty} \varphi_2(\tau) e^{-j2\pi f\tau} d\tau \\ &= \sum_{k=-\infty}^{\infty} G(f, kT_e) e^{-j2\pi kTf}\end{aligned}\quad (6)$$

where

$$G(f, kT_e) = \int_{-\infty}^{\infty} q_T(\tau) \varphi(\tau, kT_e) e^{-j2\pi f\tau} d\tau. \quad (7)$$

If we let

$$H(f, \nu) = \int_{-\infty}^{\infty} G(f, \sigma) e^{-j2\pi \nu \sigma} d\sigma \quad (8)$$

then

$$G(f, kT_e) = \int_{-\infty}^{\infty} H(f, \nu) e^{j2\pi kT_e \nu} d\nu. \quad (9)$$

Now substituting (9) into (6) and using the identity

$$\sum_{k=-\infty}^{\infty} e^{-j2\pi kx} = \sum_{m=-\infty}^{\infty} \delta(x - m) \quad (10)$$

we get

$$\Phi_2(f) = \frac{1}{T_e} \sum_{m=-\infty}^{\infty} H\left(f, \frac{T}{T_e} \left(f - \frac{m}{T}\right)\right). \quad (11)$$

Again considering typical picture material,  $\varphi(\tau, 0)$  is narrow compared to  $q_T(\tau)$  so a good approximation is  $q_T(\tau)\varphi(\tau, 0) \cong \varphi(\tau, 0)$ . In this case,  $H(f, \nu)$  is essentially just the double Fourier transform of the picture autocovariance function

$$H(f, \nu) \cong \iint_{-\infty}^{\infty} \varphi(\tau, \sigma) e^{-j2\pi(f\tau + \nu\sigma)} d\tau d\sigma. \quad (12)$$

A more significant consequence of the correlation in typical picture material is that  $\Phi_2(f)$  can be closely approximated by the product of

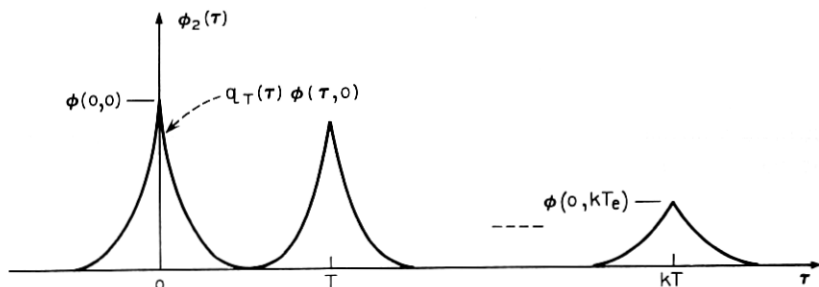


Fig. 1 — Autocorrelation of video signal with line-to-line correlation.



two functions, one periodic  $1/T$  and the other an envelope with relatively small variation over  $1/T$  intervals. Since, for typical picture material,  $H(f,0)$  and  $H(0,f)$  have roughly the same width and since  $T/T_e \gg 1$ , it follows that  $H(0, (Tf/T_e))$  is very narrow compared to  $H(f,0)$ . Furthermore, since  $H(f,0)$  has relatively small variation over an interval of width  $1/T$ , then (11) can be approximated by

$$\begin{aligned}\Phi_2(f) &\cong \frac{1}{T_e} \sum_{m=-\infty}^{\infty} H\left(\frac{m}{T}, \frac{T}{T_e} \left(f - \frac{m}{T}\right)\right) \\ &\cong \frac{1}{T_e} H(f,0) \sum_{m=-\infty}^{\infty} H\left(0, \frac{T}{T_e} \left(f - \frac{m}{T}\right)\right).\end{aligned}\quad (13)$$

A power spectral density of the form indicated in (13) corresponds to the property of separability in  $\varphi(\tau, \sigma)$ . Let

$$\varphi(\tau, \sigma) = \bar{d}^2 \varphi_h(\tau) \varphi_v(\sigma) \quad (14)$$

where  $\varphi_h(\tau)$  and  $\varphi_v(\sigma)$  are normalized autocorrelation functions for scanning along horizontal and vertical lines, respectively.  $\varphi_h(0) = \varphi_v(0) = 1$ ;  $\bar{d}^2 = \varphi(0,0)$ . Neglecting edge effects, from (12) we have

$$H(f, \nu) = \bar{d}^2 \Phi_h(f) \Phi_v(\nu),$$

and the power spectral density (11) becomes

$$\Phi_2(f) = \frac{\bar{d}^2}{T_e} \Phi_h(f) \sum_{m=-\infty}^{\infty} \Phi_v\left(\frac{T}{T_e} \left(f - \frac{m}{T}\right)\right). \quad (15)$$

A sketch of this function is shown in Fig. 2.

The final step in characterizing the effects of the scanning operation

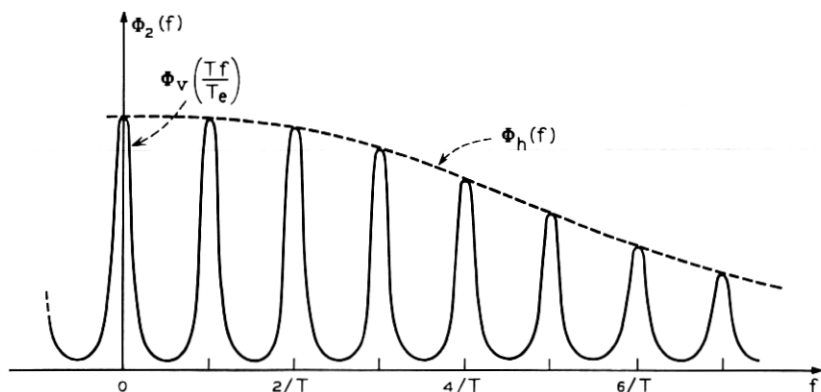


Fig. 2 — Power spectral density of video signal with line-to-line correlation.

is to account for frame-to-frame correlation in repeated scanning of a finite portion of the infinite strip. Of course, if the picture is still, the resulting process is periodic. We consider a randomly moving picture with slow variation compared to the frame repetition rate,  $1/NT$ , where vertical scanning is accomplished by  $N$  uniformly spaced lines. The nonstationarity arising from the abrupt change of scanner position when it reaches the bottom edge of the picture is handled in the same manner as before in terms of a shaping function,  $q_{NT}(\tau)$ , whose effect can be neglected for typical picture material. Expressing the normalized correlation of the luminance of a picture point at times separated by  $k$  frame intervals by  $\varphi_t(kNT)$ ;  $\varphi_t(0) = 1$ , then

$$\varphi_3(\tau) = \sum_{k=-\infty}^{\infty} \varphi_t(kNT) \varphi_2(\tau - kNT). \quad (16)$$

Because of the slow variation due to motion, frame-to-frame correlation is high and  $\varphi_3(\tau)$  is essentially the product of  $\varphi_t(\tau)$  and a periodic repetition of  $\varphi_2(\tau)$  as indicated in Fig. 3.

The power spectral density, obtained from (16) and the use of relation (10) is

$$\begin{aligned} \Phi_3(f) &= \Phi_2(f) \sum_{k=-\infty}^{\infty} \varphi_t(kNT) e^{-j2\pi kNTf} \\ &= \frac{1}{NT} \Phi_2(f) \sum_{m=-\infty}^{\infty} \Phi_t\left(f - \frac{m}{NT}\right). \end{aligned} \quad (17)$$

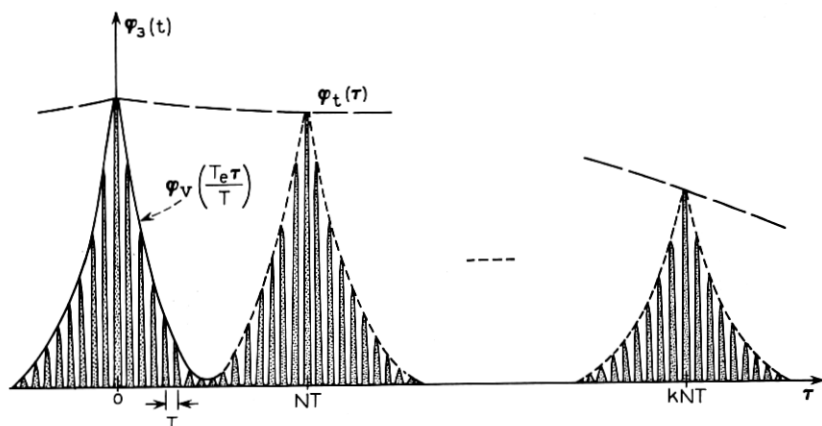


Fig. 3 — Autocorrelation of video signal with frame-to-frame correlation.

Combining (17) and (15), the final expression for  $\Phi_s(f)$  is given as the product of three functions; an envelope  $G_h(f)$  representing horizontal picture correlation, a function  $G_v(f)$ , periodic  $1/T$ , representing vertical picture correlation, and a function  $G_t(f)$ , periodic  $1/NT$ , representing frame-to-frame correlation.

$$\begin{aligned}\Phi_s(f) &= [\bar{d}^2 \Phi_h(f)] \left[ \frac{1}{T_e} \sum_{m=-\infty}^{\infty} \Phi_v \left( \frac{T}{T_e} \left( f - \frac{m}{T} \right) \right) \right] \\ &\quad \cdot \left[ \frac{1}{NT} \sum_{l=-\infty}^{\infty} \Phi_t \left( f - \frac{l}{NT} \right) \right] \quad (18) \\ &= G_h(f) G_v(f) G_t(f).\end{aligned}$$

As indicated in Fig. 4, the factors  $G_v(f)$  and  $G_t(f)$  impose a "fine structure" on  $\Phi_s(f)$ . In considering various smoothed versions of power spectral density, it is helpful to note that the average values of  $G_v(f)$  and  $G_t(f)$  are both unity.

Some practical scanning operations involve line interlacing. For the conventional 2:1 interlace scan, the resulting modification of (18) is simple. Since consecutive lines are now twice as far apart, the factor  $G_v(f)$  is modified by replacing  $T_e$  with  $2T_e$ . This modification results in the individual peaks in  $G_v(f)$  centered at multiples of  $1/T$  being broadened to twice their original width. Since the picture is scanned vertically every  $NT/2$  seconds, the  $G_t(f)$  factor is modified by replacing  $N$  by  $N/2$ . This effects a suppression of the terms centered at odd

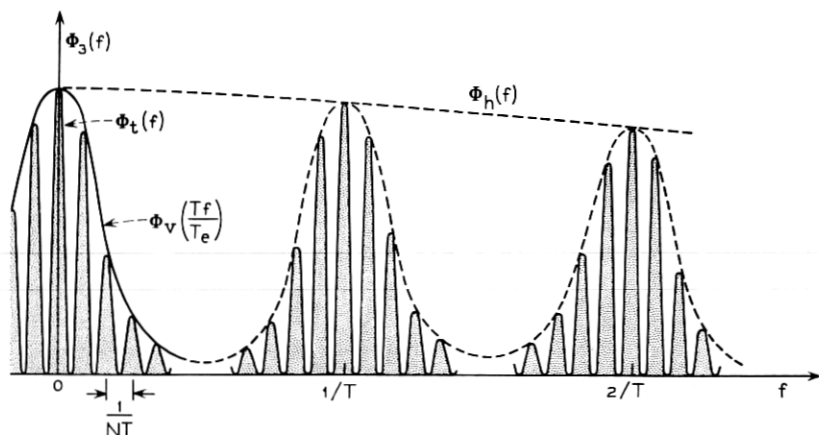


Fig. 4—Power spectral density of video signal with frame-to-frame correlation.

multiples of  $1/NT$ . This latter modification is approximate since consecutive vertical scans are not exactly in register, however the ratio of power at odd multiples of  $1/NT$  to power at even multiples of  $1/NT$  is given by the ratio of  $1 - \varphi_v(T_e)$  to  $1 + \varphi_v(T_e)$  which for typical picture material may be less than 0.01. Derivation of the modifications for more complicated interlacing arrangements is straightforward.

### III. COMPOSITE VIDEO SIGNAL

It is common practice to interrupt the video signal after each line scan and frame scan for the purpose of inserting control signals such as synchronizing and blanking pulses. The resulting signal is referred to as the composite video signal and the following development shows the form of the power spectral density. In order to simplify the argument, consider the following composite signal,  $z(t)$ , which is a random process interrupted every  $T$  seconds for a duration of  $\alpha T$  seconds with an arbitrary periodic pattern,  $w(t)$ , inserted in the blank interval:

$$z(t) = p(t) v(t) + w(t) \quad (19)$$

where  $p(t)$  is periodic  $T$ , equal to zero in the blank interval and equal to one in the video interval;  $w(t)$  is periodic  $T$  and equal to zero in the video interval; and  $v(t)$  is a zero-mean random process with autocorrelation,  $\varphi(\tau)$ . The process  $p(t) v(t)$  is, of course, nonstationary but after averaging its autocorrelation function,  $\psi(t, \tau)$ , over the period  $T$  we have

$$\begin{aligned} \bar{\varphi}(\tau) &= E [\psi(t, \tau)] \\ &= \varphi(\tau) \Pr [t \text{ and } t + \tau \text{ in video region}] \\ &= (1 - \alpha) \varphi(\tau) \sum_{k=-\infty}^{\infty} q_{(1-\alpha)\tau}(\tau - kT) \end{aligned} \quad (20)$$

where

$$\begin{aligned} q_{(1-\alpha)\tau}(\tau) &= 1 - \frac{|\tau|}{(1 - \alpha)T} \quad \text{in } |\tau| \leq (1 - \alpha)T \\ &= 0 \quad \text{otherwise.} \end{aligned}$$

From (20), the autocorrelation function of the periodically blanked process is obtained by multiplying the autocorrelation of the original process by a periodic function having a shape as indicated in Fig. 5. Note that no periodic components are generated by blanking. For moderately small  $\alpha$  and typical video signal autocorrelation functions,

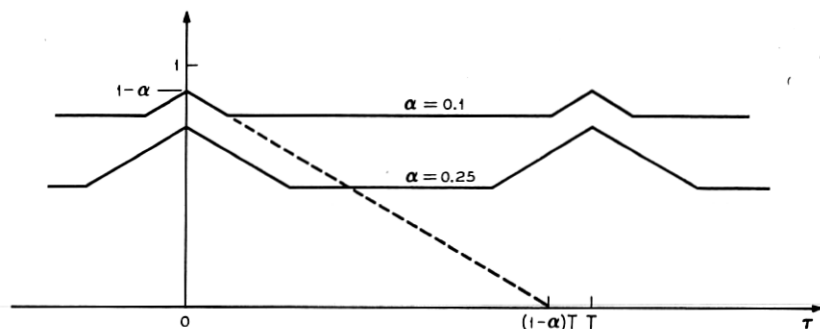


Fig. 5—Periodic shaping for autocorrelation function of periodically blanked video process.

the effect of multiplying by the periodic shaping function is essentially the same as multiplying by the constant,  $1 - \alpha$ . The power in the composite signal is the sum of the power in the blanked process and the power in the added periodic signal since  $p(t)v(t)w(t) \equiv 0$ . Hence, the power spectral density for the composite signal is

$$\Phi_z(f) = (1 - \alpha)\Phi(f) + \sum_l |w_l|^2 \delta\left(f - \frac{l}{T}\right) \quad (21)$$

where the  $w_l$  are the Fourier coefficients for  $w(t)$ . Modification of (21) for the actual control signal which consists of both horizontal and vertical synchronizing and blanking pulses is straightforward. In this case,  $w(t)$  is replaced by a signal periodic  $NT$  (or  $NT/2$  for 2:1 interlace). The constant  $1 - \alpha$  is still just the relative amount of time devoted to the video signal.

#### IV. MODEL FOR RANDOM PICTURE

To complete the model for the random video signal it remains to characterize the luminance process,  $d(x, y)$ , in such a manner that a useful expression for its autocovariance,  $\varphi(\alpha, \beta)$ , can be derived. The discussion in Section II indicated the validity of the separable form (14) for  $\varphi(\alpha, \beta)$ . Assuming separability, we need only model the one-dimensional process resulting from a unit velocity, linear scanning of the picture. Assume that a realization of this process is a piecewise-constant function,  $v(t)$ , which takes on the value  $v_n$  over the interval,  $t_n \leq t < t_{n+1}$  as shown in Fig. 6. The occurrence of the sequence  $\{t_n\}$  of points along the  $t$ -axis is a stationary random process and the sequence

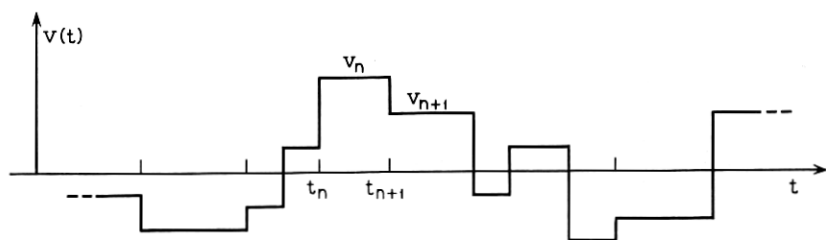


Fig. 6 — Random video signal.

$\{v_n\}$  of random variables is also stationary. Then the autocorrelation function for  $v(t)$  is

$$\varphi(\tau) = \bar{d}^2 \sum_{m=0}^{\infty} r_m P(m, \tau) \quad (22)$$

where

$$\bar{d}^2 r_m = E[v_n v_{n+m}]$$

$$\bar{d}^2 = E[v_n^2]; \quad E[v_n] = 0$$

and  $P(m, \tau)$  is the probability that the points  $t$  and  $t + \tau$  are in intervals  $m$  apart, i.e., that  $m$  points of the  $\{t_n\}$  sequence lie between them.

The simplest model is constructed by assuming that the  $\{v_n\}$  are statistically independent and that the  $\{t_n\}$  are generated by a Poisson process with rate parameter,  $\lambda$ . This model is the random step function discussed by Laning and Battin.<sup>5</sup> For this case, (22) reduces to

$$\varphi(\tau) = \bar{d}^2 P(0, \tau) \quad (23)$$

with

$$P(m, \tau) = \frac{(\lambda |\tau|)^m}{m!} e^{-\lambda |\tau|}$$

hence,

$$\varphi(\tau) = \bar{d}^2 e^{-\lambda |\tau|}. \quad (24)$$

An obvious step in the generalization of this model is to consider correlation in the  $\{v_n\}$  sequence. Suppose  $\{v_n\}$  is a stationary, wide-sense Markoff sequence.<sup>6</sup> Then it has the property that

$$r_m = r_1^m \quad (25)$$

where  $r_1$  is the correlation between adjacent elements of the sequence. In this case,

$$\begin{aligned}\varphi(\tau) &= \bar{d}^2 \sum_{m=0}^{\infty} \frac{(\lambda |\tau|)^m}{m!} r_1^m e^{-\lambda|\tau|} \\ &= \bar{d}^2 \exp [-(1-r_1)\lambda |\tau|],\end{aligned}\quad (26)$$

hence, this model is equivalent to the previous one (24) with  $\lambda$  replaced by  $(1-r_1)\lambda$ . This result suggests an interesting alternate formulation of the model. Suppose that the  $\{t_n\}$  sequence is uniformly spaced with separation  $T_e$  (stationarity is accomplished by randomizing the phase of the sequence). For this case,

$$P(m, \tau) = q_{T_e}(\tau - mT_e) + q_{T_e}(\tau + mT_e) \quad (27)$$

where

$$\begin{aligned}q_{T_e}(\tau) &= 1 - \frac{|\tau|}{T_e} \quad \text{in } |\tau| \leq T_e \\ &= 0 \quad \text{otherwise.}\end{aligned}$$

Let  $\{v_n\}$  be a stationary, wide-sense Markoff sequence with correlation  $\rho$  between adjacent elements, then

$$\begin{aligned}\varphi(\tau) &= \bar{d}^2 \sum_{l=-\infty}^{\infty} \rho^{|l|} q_{T_e}(\tau - lT_e) \\ &\cong \bar{d}^2 \exp(-\hat{\lambda} |\tau|) \quad \text{where } \hat{\lambda} = -\frac{\ln \rho}{T_e}.\end{aligned}\quad (28)$$

This is a polygonal approximation to the exponential function which, since correlation between points  $T_e$  apart is typically very large, is a very close approximation.

Using the preceding models, which are all equivalent, the random picture is characterized by an autocovariance

$$\varphi(\tau, \sigma) = \bar{d}^2 \exp(-\lambda_h |\tau| - \lambda_v |\sigma|) \quad (29)$$

which depends only on the variance,  $\bar{d}^2$ , of luminance and two parameters  $\lambda_h$  and  $\lambda_v$  which specify the average number of statistically independent luminance levels in a unit distance along the horizontal and vertical, respectively. Alternatively, the correlation is characterized by the parameters  $\rho_h = \exp[-\lambda_h T_e]$  and  $\rho_v = \exp[-\lambda_v T_e]$  which are the correlation coefficients of luminance in adjacent picture elements when the picture area is quantized into small squares of dimension  $T_e$ .

The suitability of the exponential correlation function for modeling the random picture can be established by examining the results of

correlation measurements reported by Kretzmer<sup>1</sup> and O'Neal<sup>2</sup> and power spectral density measurements by Deriugin.<sup>3</sup>

## V. SUMMARY

Combining the results of the preceding sections, simple closed-form expressions can be written for the power spectral density of the composite video signal. At this point the mean value  $\bar{d}$  of the luminance is included so the variance of the luminance becomes  $\bar{d}^2 - \bar{d}^2$ . The synchronizing and blanking signals are assumed to occupy a fraction  $\alpha$  of the total time and to form a pattern periodic  $NT$ . Let  $w_l$  be the Fourier coefficients of the periodic signal added to  $\bar{d}$  in the blank intervals. Then the power spectral density for the composite signal is

$$S(f) = (1 - \alpha)G_h(f)G_v(f)G_t(f) + \sum_{l=-\infty}^{\infty} |w_l|^2 \delta\left(f - \frac{l}{NT}\right) + \bar{d}^2 \delta(f). \quad (30)$$

Using the exponential correlation functions of Section IV and (18), we have

$$G_h(f) = (\bar{d}^2 - \bar{d}^2) \frac{2\lambda_h}{(2\pi f)^2 + \lambda_h^2}. \quad (31)$$

The factor indicating shaping due to line-to-line correlation becomes

$$G_v(f) = \frac{1}{T_e} \sum_{m=-\infty}^{\infty} \frac{2\lambda_v}{\left[2\pi T/T_e \left(f - \frac{m}{T}\right)\right]^2 + \lambda_v^2}. \quad (32)$$

The closed form for this expression is obtained by noting that  $G_v(f)$  is the convolution product,

$$G_v(f) = \frac{T}{T_e} \frac{2\lambda_v}{(2\pi T f / T_e)^2 + \lambda_v^2} * \frac{1}{T} \sum_m \delta\left(f - \frac{m}{T}\right). \quad (33)$$

Using the identity (10) and performing the indicated convolution,  $G_v(f)$  is expressed as a geometric series which can be summed to give

$$G_v(f) = \frac{\sinh T_e \lambda_v}{\cosh T_e \lambda_v - \cos 2\pi T f}. \quad (34)$$

A similar expression for the  $G_t(f)$  factor can be obtained by assuming that luminance of a point at successive frames forms a wide-sense Markoff sequence with frame-to-frame correlation  $\rho_t = \exp[-\lambda_t NT]$ .



Then

$$G_t(f) = \frac{\sinh NT\lambda_t}{\cosh NT\lambda_t - \cos 2\pi NTf}. \quad (35)$$

Frame-to-frame correlation,  $\rho_t$ , has been measured experimentally<sup>1</sup> and found to lie between 0.86 and 0.80 for typical material. Using these values in (35) the width (between  $-3$ -db points) of the peaks in  $G_t(f)$  is only about 0.048 to 0.071 of the separation,  $1/NT$ , between the peaks.

In applications where the structure of  $G_t(f)$  is too fine to resolve, the smoothed version,  $(1 - \alpha)G_h(f)G_v(f)$ , of the continuous part of the power spectral density is of interest. This quantity is shown in Fig. 7 for two different types of video signal; one the standard 525-line, 30-frame per second broadcast television signal (BCTV) and the other the 275-line, 30-frame per second, initial design of the Bell System station-to-station *Picturephone*® service (PP). For comparison, it is assumed that both pictures have the same correlation,  $\rho = 0.9$ , between picture elements of dimension  $T_e$  in both horizontal and vertical directions. Also both signals are obtained from 2:1 interlaced scanning. The difference in the two curves in Fig. 7 is due to different values of the quantity,  $T_e/T$ .  $T_e/T$  is a fundamental parameter of the raster design depending

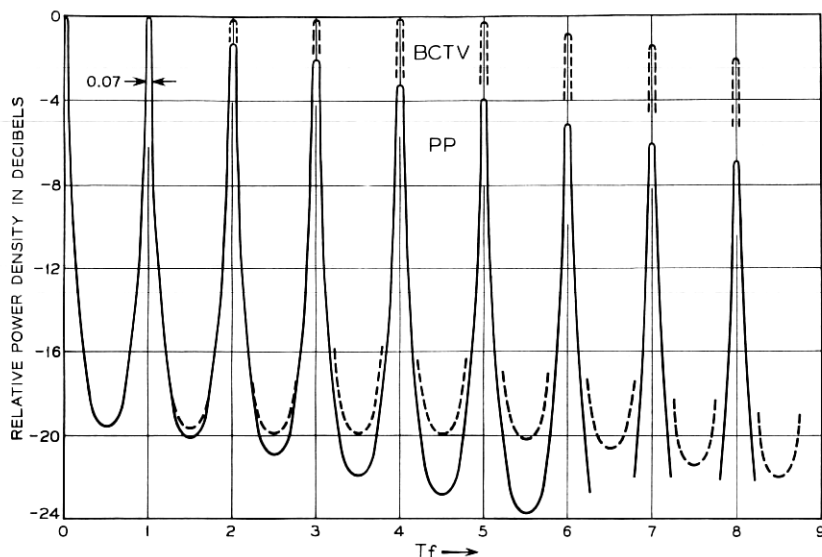


Fig. 7 — Continuous part of power spectral density for two typical video signals with frame rate structure smoothed out. ( $\rho = \rho_h = \rho_v = 0.9$ .)

on the number of lines per frame, the aspect ratio of the visible portion of the picture, and the relative size of the blank portions of the horizontal and vertical scans. For BCTV,  $T_e/T = 0.00128$ ; and for PP,  $T_e/T = 0.0041$ .

The value of the parameter  $\rho$  used in Fig. 7 represents a highly detailed random picture. A typical head-and-shoulders view of a person may have  $\rho = 0.99$  and  $\rho = 0.98$  represents a moderately detailed picture.<sup>1</sup> Even for  $\rho = 0.9$  the power is extremely concentrated around multiples of the line scan rate,  $1/T$ . The width of the peaks between  $-3$ -db points and also the ratio between successive maxima and minima in the power density are shown in Table I for various values of  $\rho$  and  $\lambda T_e$ .

## VI. APPLICATION

One obvious application of the model is in problems concerning minimum mean-squared error filtering of the video signal in noise. Solution of these problems invariably requires a knowledge of power spectral densities of the signal and noise. The concept of utilizing the inherent redundancy in the video signal to ease transmission requirements is familiar. Alternative to seeking coding arrangements which reduce bandwidth requirements, we can consider linear processing operations which utilize the highly nonuniform nature of the power spectral density to effect a reduction of signal power needed for a given performance.

As an example of this approach, consider the design of optimum pre-emphasis and de-emphasis filters for transmission over a noisy channel as shown in Fig. 8. Assume that the channel has a constraint on maximum signal power and that it is desired to minimize mean-squared error in the received signal,  $y(t)$ .

Details of the derivation of the optimum filtering characteristics

TABLE I — WIDTH AND HEIGHT OF POWER DENSITY CONCENTRATIONS ABOUT MULTIPLES OF THE LINE SCANNING RATE FOR 2:1 INTERLACED SCANNING

$\rho$	$\lambda T_e = -\ln \rho$	Width (between $-3$ db Points) Relative to $1/T$	$10 \log_{10} \frac{S(n/T)}{S(n + \frac{1}{2}T)}$
0.99	0.010	0.00636	40.0 db.
0.98	0.020	0.0127	34.0
0.97	0.030	0.0191	30.4
0.95	0.051	0.0326	25.8
0.90	0.105	0.0668	19.6
0.85	0.163	0.1035	15.8
0.80	0.223	0.1420	13.2

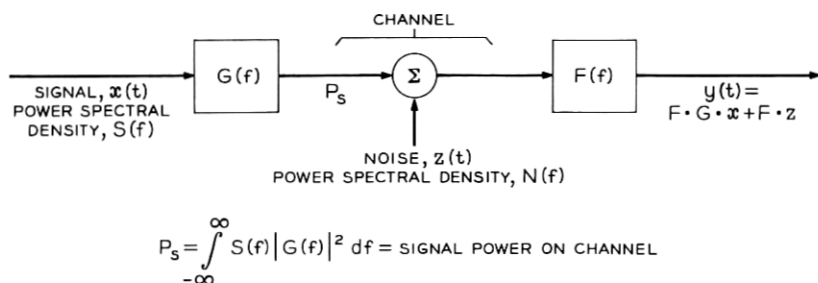


Fig. 8 — Spectrum shaping for transmission over noisy channel.

are presented in Appendix B. For high signal-to-noise ratio on the channel, the two filters are essentially inverse and we get\*

$$F(f) = G^{-1}(f) = \left[ \frac{\mu S(f)}{N(f)} \right]^{\frac{1}{2}} \quad (36)$$

where the constant  $\mu$  is adjusted to meet the signal power constraint.

$$\mu^{\frac{1}{2}} = \frac{1}{P_s} \int (SN)^{\frac{1}{2}} df. \quad (37)$$

The advantage gained by using the filter networks can be expressed as a signal-to-noise ratio improvement factor  $\gamma$  which is simply the ratio of signal-to-noise ratios at the output of the receiver with and without filtering.

$$\gamma = \frac{\int S df \int N df}{\int S F^{-2} df \int N F^2 df}. \quad (38)$$

When the optimum filter pair (36) is used, (38) becomes

$$\gamma_{\text{opt}} = \frac{\int S df \int N df}{[\int (SN)^{\frac{1}{2}} df]^2}. \quad (39)$$

The expression for  $\gamma_{\text{opt}}$  provides another interesting measure of the nonuniformity of  $S(f)$ . In a function space representation, the quantity,  $\cos^{-1} (1/\gamma_{\text{opt}})^{\frac{1}{2}}$ , is conventionally interpreted as the angle between the functions  $S^{\frac{1}{2}}(f)$  and  $N^{\frac{1}{2}}(f)$ . If we consider flat noise over a band  $W$  and zero outside, then  $\gamma_{\text{opt}}$  becomes a comparison of  $S^{\frac{1}{2}}(f)$  with a con-

\* The expressions for  $S(f)$  use only the continuous part of the expression. The discrete components should not be transmitted in this problem.

stant over the band of interest. In this case,

$$\gamma_{\text{opt}} = \frac{2W \int S df}{\left[ \int_{-W}^W S^{\frac{1}{2}} df \right]^2}. \quad (40)$$

Values of  $\gamma_{\text{opt}}$  in (40) are plotted in Fig. 9 for the case,  $W = 60/T$  and  $T_e/T = 0.0041$ ; these parameters corresponding to the *Picture-phone* video signal.

The form of the optimum filter, in this case  $F(f) = S^{\frac{1}{2}}(f)$ , suggests a rather difficult realization problem. Accordingly, it is interesting to evaluate the performance of a suboptimum filter pair having the simple form shown in Fig. 10. The parameter,  $a$ , in the network realizing the periodic part of the transfer function is adjusted to match the maxima and minima in  $S^{\frac{1}{2}}(f)$ . The values of  $\gamma$  using this filter pair are also shown on Fig. 9 and are seen to be remarkably close to the optimum values. It is of interest to note that part of the pre-emphasis filter effects a smoothing of the transmitted power spectral density by transmitting only the partial difference,  $x(t) - ax(t - T)$ , between successive lines. This technique has been discussed by Harrison<sup>7</sup> and O'Neal<sup>2</sup> with regard

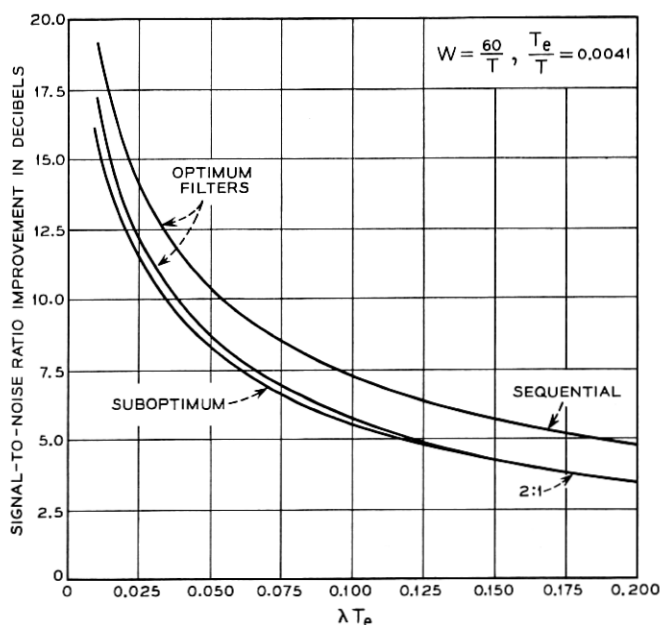


Fig. 9 — Performance of spectrum shaping filters. ( $W = 60/T$ ,  $T_e/T = 0.0041$ .)

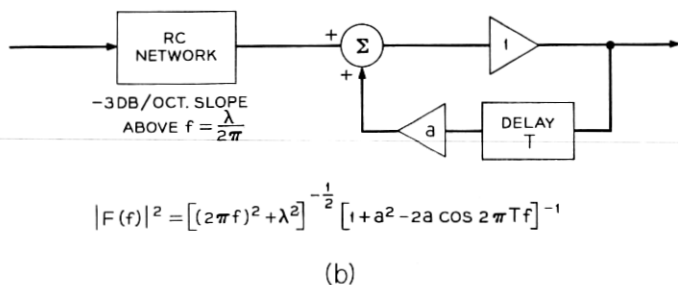
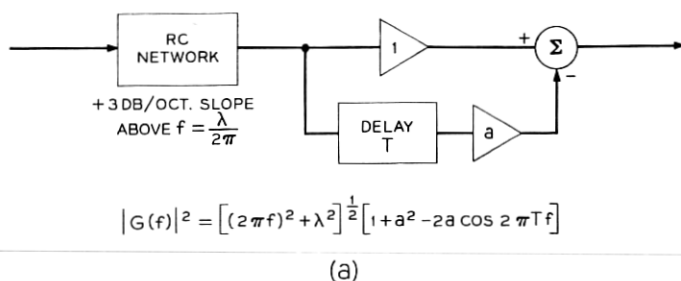


Fig. 10—Suboptimum filter pair; (a) pre-emphasis network, (b) de-emphasis network.

to the use of “previous line” linear prediction to reduce the correlation present in the transmitted signal.

In actual practice, a substantial portion of the indicated advantage may not be realizable. This is because the received noise, in passing through  $F(f)$ , is concentrated at multiples of  $1/T$  causing a line-to-line correlation which is subjectively more annoying than the same amount of flat noise power. This subjective effect has not yet been fully evaluated. If it can be described by a frequency domain weighting function, then the methods presented in Appendix B can be easily adapted to give a more accurate evaluation of optimum filtering.

## APPENDIX A

### Glossary of Symbols

$d(x, y)$	luminance at the point $(x, y)$ on the picture.
$\varphi(\alpha, \beta)$	autocorrelation of picture luminance.
$\varphi_1(\tau)$	autocorrelation of video signal obtained from linear horizontal scanning of infinite picture.

$\varphi_2(\tau)$	autocorrelation of video signal obtained by sequential horizontal scanning of infinite vertical strip.
$\varphi_3(\tau)$	autocorrelation of video signal obtained by repeated scanning of rectangular portion of moving picture.
$\varphi_h(\tau), \varphi_v(\tau)$	normalized versions of $\varphi(\tau, 0)$ and $\varphi(0, \tau)$ , respectively.
$\varphi_t(\tau)$	normalized autocorrelation of luminance at a point as a function of time.
$G_h(f), G_v(f), G_t(f)$	factors of the power spectral density characterizing point-to-point, line-to-line, and frame-to-frame correlation, respectively.
$S(f)$	power spectral density of composite video signal.
$w(t)$	periodic part of composite video signal less the average luminance, $\bar{d}$ .
$w_l$	$l$ th Fourier coefficient of $w(t)$ .
$\alpha$	relative amount of time occupied by non-video portion of the signal.
$T$	line scan interval in seconds.
$T_e$	time interval equivalent to distance between adjacent lines at scanner velocity.
$N$	number of lines per frame.
$\lambda_h, \lambda_v$	Poisson rate parameter describing luminance process in horizontal and vertical directions, respectively.
$\rho_h, \rho_v$	correlation between luminance values in adjacent square picture elements, of dimension $T_e$ , in horizontal and vertical directions, respectively.

## APPENDIX B

*Optimum Filtering of Random Video Signals*

The criterion for optimum performance is expressed in terms of mean-squared deviation between the received signal,  $y(t)$ , and the transmitted signal,  $x(t)$ , shown in Fig. 8. The received signal is decomposed into distorted signal component,  $u(t) = FG \cdot x(t)$ , and noise component,  $v(t) = F \cdot z(t)$ .

Let

$$\begin{aligned}
 I &= E [(x - y)^2] \\
 &= E [(x - u)^2] + E [v^2] - 2E [(x - u)v].
 \end{aligned}
 \tag{41}$$

The last term in (41) vanishes by assuming statistical independence of signal and noise and zero-mean for the noise. The two remaining functionals are expressed in the frequency domain as

$$I = \int S(f) |1 - F(f)G(f)|^2 df + \int N(f) |F(f)|^2 df. \quad (42)$$

We want to find the filter transfer functions  $F(f)$  and  $G(f)$  such that  $I$  is minimized subject to the constraint on signal power on the channel.

$$\int S(f) |G(f)|^2 df = P_s. \quad (43)$$

Problems of this type appear to have been first discussed by Costas.<sup>8</sup> It can be shown that if the signal-to-noise ratio on the channel is moderately high, then  $F(f)$  and  $G(f)$  are essentially inverse. Accordingly, we add the constraint,  $G^{-1}(f) = F(f)$ , which makes the first term in (42) vanish, and find the stationary points of  $I + \mu P_s$  with respect to  $F$ .

$$I + \mu P_s = \int NF^2 df + \mu \int SF^{-2} df \quad (44)$$

where we assume  $F$  to be a real function (since its phase does not affect signal power or noise power) with the understanding that the pre-emphasis filter can have an arbitrary phase shift since the de-emphasis filter has the complementary phase shift. In order that the first variation of the functional in (44) vanish, it is necessary that

$$F^2 = \left( \frac{\mu S}{N} \right)^{\frac{1}{2}} \quad (45)$$

where

$$\mu^{\frac{1}{2}} = \frac{1}{P_s} \int (SN)^{\frac{1}{2}} df$$

in order to meet the constraint on signal power. Substituting (45) into (44) the minimum mean-squared interference becomes

$$I_{\min} = \frac{1}{P_s} \left[ \int (SN)^{\frac{1}{2}} df \right]^2. \quad (46)$$

Because of the constraint,  $G^{-1} = F$ , it makes sense to speak of signal-to-noise ratio at the output of the receiver. The improvement in signal-to-

noise ratio by choosing  $F$  according to (45) relative to  $F \equiv 1$  is expressed as

$$\gamma_{\text{opt}} = \frac{\int S df \int N df}{\left[ \int (SN)^{\frac{1}{2}} df \right]^2}. \quad (47)$$

If we assume that  $N(f)$  is constant over the band  $|f| \leq W$  and zero elsewhere, then (47) becomes

$$\gamma_{\text{opt}} = \frac{2W \int S df}{\left[ \int_{-W}^W S^{\frac{1}{2}} df \right]^2}. \quad (48)$$

Now let  $S(f)$ , as indicated in Section V with  $\lambda_h = \lambda_v = \lambda$ , be given by

$$S(f) = K \left[ \frac{2\lambda}{(2\pi f)^2 + \lambda^2} \right] \left[ \frac{\sinh \lambda T_e}{\cosh \lambda T_e - \cos 2\pi T f} \right]$$

and since

$$\int S(f) df = \varphi(0) = K,$$

we have

$$\gamma_{\text{opt}} = 2W \left\{ \int_{-W}^W \left[ \frac{2\lambda}{(2\pi f)^2 + \lambda^2} \right]^{\frac{1}{2}} \left[ \frac{\sinh \lambda T_e}{\cosh \lambda T_e - \cos 2\pi T f} \right]^{\frac{1}{2}} df \right\}^{-2}. \quad (49)$$

Integrals of this type, having an integrand  $A(f) B(f)$  where  $B(f)$  is periodic  $1/T$  and  $A(f)$  is a slowly changing envelope function, can be closely approximated by

$$\begin{aligned} \int_{-W}^W A(f) B(f) df &\cong \sum_{m=-WT}^{WT} A\left(\frac{m}{T}\right) \int_{1/T} B(f) df \\ &\cong T \int_{-W}^W A(f) df \int_{1/T} B(f) df. \end{aligned} \quad (50)$$

Accordingly, we evaluate

$$\int_{-W}^W \left[ \frac{2\lambda}{(2\pi f)^2 + \lambda^2} \right]^{\frac{1}{2}} df \cong \frac{(2\lambda)^{\frac{1}{2}}}{\pi} \ln \frac{4\pi W}{\lambda} \quad \text{for} \quad \frac{W}{\lambda} \geq 1$$



and using a suitable change of variable on the second integral

$$\int_{1/T} \left[ \frac{\sinh \lambda T_e}{\cosh \lambda T_e - \cos 2\pi T f} \right]^{\frac{1}{2}} df = \frac{2}{\pi T} \tanh^{\frac{1}{2}} \frac{\lambda T_e}{2} \int_0^{\pi/2} \frac{d\varphi}{[1 - k^2 \sin^2 \varphi]^{\frac{1}{2}}}$$

where

$$k^{-1} = \cosh \frac{\lambda T_e}{2}.$$

This last integral is recognized as the complete elliptic integral of the first kind,  $\mathcal{K}(\sin^{-1} k)$ , which can be obtained from tables. Now combining these results,

$$\left[ \int_{-W}^W S^{\frac{1}{2}} df \right]^2 = \frac{8\lambda}{\pi^4} \tanh \frac{\lambda T_e}{2} \left[ \ln \frac{4\pi W}{\lambda} \right]^2 \mathcal{K}^2(\sin^{-1} k) \quad (51)$$

and (49) becomes

$$\gamma_{\text{opt}}(\lambda) = \frac{\frac{\pi^4 W}{4\lambda}}{\tanh \frac{\lambda T_e}{2} \left[ \ln \frac{4\pi W}{\lambda} \right] \mathcal{K}^2(\sin^{-1} k)}. \quad (52)$$

This function is plotted in Fig. 9 over the range of typical values of  $\lambda$ .

For the suboptimum filters shown in Fig. 10, we want to evaluate  $\gamma$  in (38) for the flat noise case. The integrals are evaluated using the approximation indicated in (50).

$$\gamma(\lambda) = \frac{\pi^2 (W/\lambda)}{\frac{1}{1-a^2} \left[ \ln \frac{4\pi W}{\lambda} \right]^2 [1 + a^2 - 2ae^{-\lambda T_e}]}. \quad (53)$$

In (53) the parameter  $a$  is selected to satisfy

$$(1 - a/1 + a)^2 = \tanh \lambda T_e/2. \quad (54)$$

This choice of  $a$  makes the ratio of maxima to minima in the periodic part of the transfer function equal to that of the optimum filter. Values of  $\gamma(\lambda)$  from (53) with  $T_e$  replaced by  $2T_e$  for 2:1 interlace scanning are also shown on Fig. 9.

#### REFERENCES

1. Kretzmer, E. R., Statistics of Television Signals, B.S.T.J., 31, July, 1952, pp. 751-763.
2. O'Neal, J. B., Predictive Quantizing Systems (Differential Pulse Code Modulation) for the Transmission of Television Signals, To be published.

3. Deriugin, N. G., The Power Spectrum and the Correlation Function of the Television Signal, *Telecommunications* #7, 1952, pp. 1-12.
4. Ignat'yev, N. K., Power Spectrum of a Signal Obtained by Scanning, *Radio Eng. Electron. Phys.*, 6, No. 1, Jan., 1961, pp. 19-23.
5. Laning, J. H. and Battin, R. H., *Random Processes in Automatic Control*, McGraw-Hill Book Co., New York, 1956, Ch. 3.
6. Papoulis, A., *Probability, Random Variables, and Stochastic Processes*, McGraw-Hill Book Co., New York, 1965, Ch. 15.
7. Harrison, C. W., Experiments with Linear Prediction in Television, *B.S.T.J.*, 31, July, 1952, pp. 764-783.
8. Costas, J. P., Coding with Linear Systems, *Proc. IRE*, 40, No. 9, Sept., 1952, pp. 1101-1103.